Hot spot generation in energetic materials created by long-wavelength infrared radiation

Ming-Wei Chen, Sizhu You, Kenneth S. Suslick, and Dana D. Dlott

Citation: Applied Physics Letters **104**, 061907 (2014); doi: 10.1063/1.4865258
View online: http://dx.doi.org/10.1063/1.4865258
View Table of Contents: http://scitation.aip.org/content/aip/journal/apl/104/6?ver=pdfcov
Published by the AIP Publishing

This article is copyrighted as indicated in the article. Reuse of AIP content is subject to the terms at: http://scitation.aip.org/termsconditions. Downloaded to IP: 130.126.229.119 On: Tue, 11 Feb 2014 17:02:01

Hot spot generation in energetic materials created by long-wavelength infrared radiation

Ming-Wei Chen, Sizhu You, Kenneth S. Suslick, and Dana D. Dlott[a)]
School of Chemical Sciences and Fredrick Seitz Materials Research Laboratory, University of Illinois at Urbana-Champaign, Urbana, Illinois 61801, USA

(Received 16 January 2014; accepted 29 January 2014; published online 11 February 2014)

Hot spots produced by long-wavelength infrared (LWIR) radiation in an energetic material, crystalline RDX (1,3,5-trinitroperhydro-1,3,5-triazine), were studied by thermal-imaging microscopy. The LWIR source was a CO_2 laser operating in the 28-30 THz range. Hot spot generation was studied using relatively low intensity ($\sim$100 W cm^{-2}), long-duration (450 ms) LWIR pulses. The hot spots could be produced repeatedly in individual RDX crystals, to investigate the fundamental mechanisms of hot spot generation by LWIR, since the peak hot-spot temperatures were kept to $\sim$30 K above ambient. Hot spots were generated preferentially beneath RDX crystal planes making oblique angles with the LWIR beam. Surprisingly, hot spots were more prominent when the LWIR wavelength was tuned to be weakly absorbed (absorption depth $\sim$30 μm) than when the LWIR wavelength was strongly absorbed (absorption depth $\sim$5 μm). This unexpected effect was explained using a model that accounts for LWIR refraction and RDX thermal conduction. The weakly absorbed LWIR is slightly focused underneath the oblique crystal planes, and it penetrates the RDX crystals more deeply, increasing the likelihood of irradiating RDX defect inclusions that are able to strongly absorb or internally focus the LWIR beam. © *2014 AIP Publishing LLC*.
[http://dx.doi.org/10.1063/1.4865258]

We report here the formation of hot spots[1–5] in energetic materials (EM), produced by 28–30 THz radiation, which may be termed "terahertz" or "long-wavelength infrared" (LWIR). The hot spots were detected with a recently developed thermal-imaging microscope.[6] The responses of EM to strong stimuli such as shock waves[7] or intense, short-duration laser pulses[8,9] have been studied for decades. EM initiation by weaker stimuli can also occur and always involves localized hot spot generation.[2] Excitation by weaker stimuli may have potential applications for the remote disabling of explosive devices; for example, one possible strategy for remotely disabling EM using LWIR involves using lower-intensity LWIR to generate smaller, colder hot spots that gradually consume the EM, avoiding the explosive reaction regime. To understand how one might achieve this goal, we have investigated the mechanism of LWIR generation of hot spots in EM. There are very few methods to directly observe EM hot spots *in situ*, and our thermal microscopy apparatus is uniquely suited for this task.

The thermal imaging microscope was previously used[6] to observe LWIR-generated hot spots in $\sim$1 mm RDX (1,3,5-trinitroperhydro-1,3,5-triazine) crystals. RDX detonates at 8.75 km s^{-1}, at a pressure of 28 GPa, with energy release of 6.3 kJ kg^{-1}.[10] The hot spots seen previously were generated by intense LWIR that created explosively growing hot spots in RDX, causing the RDX crystals to be consumed faster than the 8.3 ms interval between video frames.[6] Surprisingly, we have now found that lower-intensity LWIR produces *non-explosive hot spots*, which enables us to conduct repeated experiments on the same RDX crystals, with different LWIR wavelengths and crystal orientations.

The thermal-imaging microscope (Fig. 1) consisted of a mid-wavelength IR camera (3.7–4.8 μm, MWIR) and a 1 $\times$ IR objective that, in tandem, gave a spatial resolution of 15–20 μm. The LWIR source was a line-tunable 50 W CO_2 laser. An acousto-optic modulator was used to control the laser intensity, and an electrical shutter was used to slice pulses from the laser output. RDX crystals were sandwiched between salt (NaCl) windows, and a dichroic MWIR/LWIR beamsplitter was used to image the crystals from the same side as the LWIR irradiation.[6]

Figure 2 provides the RDX absorption spectrum (powder in KBr) in the 28–30 THz range where transitions were attributed to CH_2 bending and N-NO_2 stretching.[11] Although we studied six LWIR wavelengths (arrows in Fig. 2(a)), we will analyze our results by considering two regimes, 940–950 cm^{-1}, where LWIR was "strongly absorbed," and 970–985 cm^{-1} where LWIR was "weakly absorbed." Absorption depths (absorption coefficient α^{-1}) were 6 μm for 949.5 cm^{-1} in the strongly absorbed regime and 28 μm for 973.3 cm^{-1} in the weakly absorbed regime.

The $\sim$2 mm diameter LWIR laser beam profile varied somewhat at different wavelengths. In Fig. 2(b) we show thermal images of the LWIR beam on glass. Glass has a nearly wavelength-independent absorption in this range.[6] The thermal images are computed false-color plots of I/I_0, where I_0 was the 298 K emission intensity and I the emission intensity during LWIR irradiation. We adjusted the LWIR intensity at each wavelength to achieve the same I/I_0 at the beam center. In one thermal image in Fig. 2(b), we superimposed an optical micrograph of an RDX crystal (grown by controlled slow evaporation from acetone solution), to show

a)Author to whom correspondence should be addressed. Electronic mail: dlott@illinois.edu

 © 2014 AIP Publishing LLC

This article is copyrighted as indicated in the article. Reuse of AIP content is subject to the terms at: http://scitation.aip.org/termsconditions. Downloaded to IP: 130.126.229.119 On: Tue, 11 Feb 2014 17:02:01

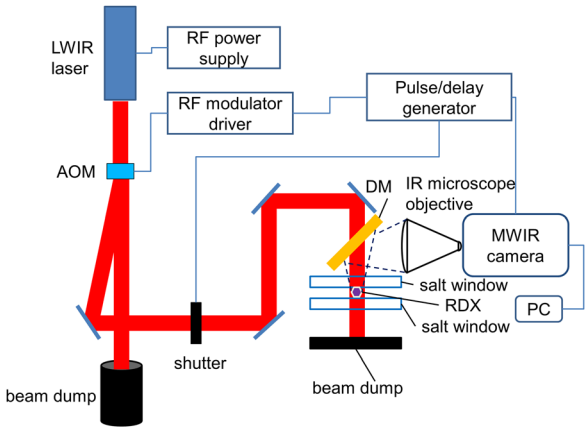

FIG. 1. Schematic of thermal imaging microscope and LWIR source. MWIR = mid-wavelength infrared; DM = dichroic mirror; AOM = acousto-optic modulator.

that the crystals were uniformly illuminated. RDX crystals had a central bright region denoting the (200) plane normal to the LWIR beam, and darker regions indicating adjacent oblique planes. We converted I/I_0 values to temperature using calibration images of RDX crystals on a resistively heated plate at several known temperatures, as described previously.[6]

In Fig. 3, we show thermal images of four LWIR-irradiated RDX crystals with the (200) faces normal to the LWIR beam, acquired using 450 ms, 3.5 W LWIR pulses, with 100 μs image acquisition times. To the left of each row of thermal images, we placed an optical micrograph of each crystal, digitally sized and rotated to match the thermal images. The 3.5 W LWIR power level was selected to keep the peak temperature jumps in RDX below 30 K, which produced readily observed hot spots but which did not appear to damage RDX. Figure 3 shows a remarkable result: *hot spots were more prominent in the cases where the LWIR was weakly absorbing (i.e., rightmost four columns)*. Figure 4 shows two RDX crystals heated by strongly absorbed or

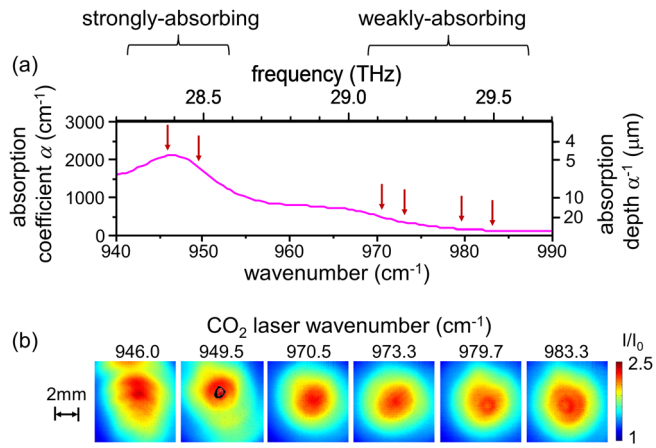

FIG. 2. (a) LWIR absorption spectrum of RDX. Arrows indicate wavelengths used to pulse-irradiate RDX. (b) Thermal images of the LWIR beam on glass. In the 949.5 cm^{-1} panel, an optical micrograph of a typical RDX crystal was superimposed on the uniformly illuminated region in the beam center. The bright central region of RDX was the (200) plane normal to the LWIR beam, and the darker regions were adjacent oblique planes, as seen more clearly on the left-hand side of Fig. 3.

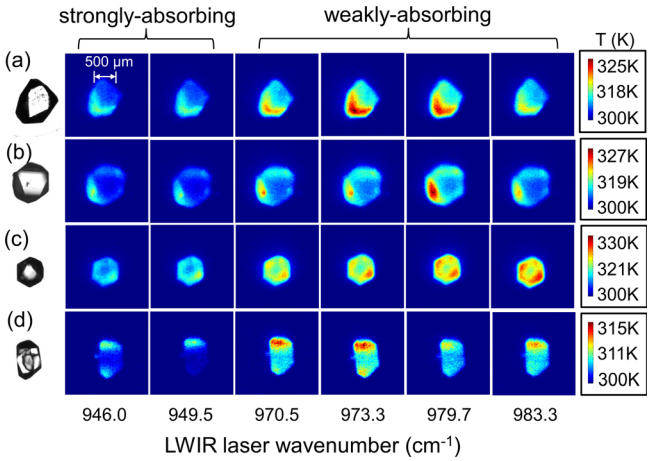

FIG. 3. (a)–(d) Thermal images of RDX crystals irradiated for 450 ms by 3.5 W LWIR pulses at the indicated wavenumbers. To the left of each row is an optical micrograph of each RDX crystal. Hot spots were associated with the oblique planes of the RDX crystals and were much more prominent with weakly absorbed LWIR irradiation, than with the strongly absorbed LWIR.

weakly absorbed LWIR, as crystals were rotated around the azimuth. Although hot spot temperatures varied with azimuthal angle, the hot spots were always created in the same parts of the crystal. Hot spots were created *in regions associated with the oblique crystal planes*, i.e., those crystal planes making obtuse angles with the LWIR beam.

Thus we see that hot spots are most prominent in the oblique crystal planes with weakly absorbed irradiation.

We can qualitatively explain these results using simple models for light interactions with absorbing slabs described in Fig. 5.

First consider a spatially uniform laser beam with intensity I incident on an RDX slab having absorption coefficient α and heat capacity C. The laser is turned on at $t = 0$ and the RDX surface is $z = 0$. A one-dimensional model can be used for the adiabatic temperature profile $\Delta T_a(z,t)$[12]

$$\Delta T_a(z,t) = \frac{I\alpha t}{C}\exp(-\alpha z). \quad (1)$$

Equation (1) shows that strongly absorbed light (larger α) would normally be expected to produce higher temperatures.

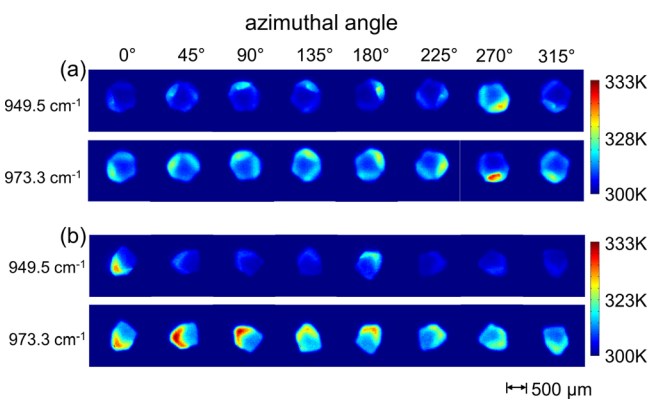

FIG. 4. Thermal images of two RDX crystals irradiated with 949.5 cm^{-1} (strongly absorbed LWIR) and 973.3 cm^{-1} (weakly absorbed LWIR), with azimuthal rotation. Although the hot spot temperatures depend on rotation angle, the hot spot locations do not. Hot spots are associated with the oblique planes of the RDX crystals.

This article is copyrighted as indicated in the article. Reuse of AIP content is subject to the terms at: http://scitation.aip.org/termsconditions. Downloaded to IP: 130.126.229.119 On: Tue, 11 Feb 2014 17:02:01

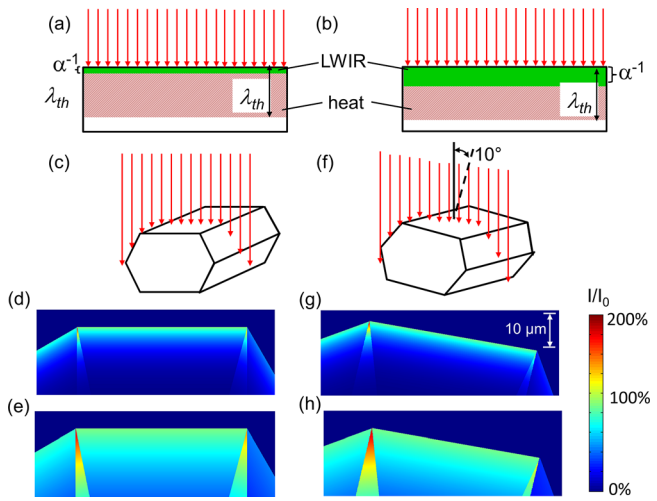

FIG. 5. Models for LWIR irradiation of RDX slabs. (a) Strongly absorbed and (b) weakly absorbed regimes. During the 450 ms duration LWIR pulses, the RDX slabs were heated the same amount and to the same depth (λ_{th}) in both regimes, but LWIR penetrated more deeply into RDX in the weakly absorbed regime. Models for LWIR refraction by a slab (c) with a plane normal to the LWIR beam, or (f) tilted 10° off the beam axis, both with oblique planes at 150° and 120°. In the strongly absorbed regime, the absorption depth $\alpha^{-1} = 5\,\mu$m. In the weakly absorbed regime $\alpha^{-1} = 25\,\mu$m. (d) Computed LWIR intensity inside RDX in the strongly absorbed regime. (e) LWIR intensity in the weakly absorbed regime. (f) LWIR intensity inside tilted RDX in the strongly absorbed regime. (h) LWIR intensity in the tilted RDX in the weakly absorbed regime. The LWIR intensity is concentrated where the flat and oblique planes meet, and the concentration effect is greater in the weakly absorbed regime.

Therefore our results showing hot spots more prominent with weakly absorbed light were surprising, and the mechanism is novel and interesting.

With thermal diffusion the temperature profile can be computed using the one-dimensional Green's function

$$\Delta T(z,t) = \int_0^t dt' \int_0^\infty dz' \Delta T_a(z',t') \frac{1}{[4\pi D(t-t')]^{1/2}} \times \exp\left[-\frac{(z-z')^2}{4D(t-t')}\right], \quad (2)$$

where D is the thermal diffusivity.

A simple interpretation of Eq. (2) describes the heat distribution in the RDX slab in terms of absorption depth α^{-1} and thermal diffusion length λ_{th}, where

$$\lambda_{th} = \frac{1}{2}\sqrt{2Dt}. \quad (3)$$

Equation (1) is valid when thermal diffusion is minimal, $\lambda_{\text{th}} \ll \alpha^{-1}$. In that case RDX is heated to a depth α^{-1} and the surface temperature $\Delta T(0,t)$ is proportional to α. Equation (2) is needed, and thermal diffusion is dominant, when $\lambda_{th} \gg \alpha^{-1}$. In that case RDX is heated to a depth λ_{th}, and the surface temperature is proportional to ${\lambda_{th}}^{-1}$ and independent of α.

For RDX, based on studies of tightly compacted powders,[13] $D \approx 1 \times 10^{-3}\,\text{cm}^2\,\text{s}^{-1}$. With 450 ms LWIR pulses, $\lambda_{th} = 150\,\mu$m, so λ_{th} significantly exceeds the absorption depths of either the strongly absorbed LWIR ($\alpha^{-1} = 6\,\mu$m) or the weakly absorbed LWIR ($\alpha^{-1} = 28\,\mu$m). As illustrated in Figs. 5(a) and 5(b), in this case the heat distributions and surface temperatures will be almost identical with strongly absorbed and weakly absorbed LWIR, but the weakly absorbed LWIR will penetrate RDX about four times more deeply.

We did a simple simulation to demonstrate the refraction effects of oblique RDX crystal facets. The refractive index n_{RDX} is 1.6,[1] and we ignored diffraction and the ~4% reflections from RDX surfaces. The LWIR was collimated and directed to a normal-incidence RDX surface bounded by oblique planes making angles of 150° and 120° to the normal, as illustrated in Fig. 5(c). We did simulations with $\alpha^{-1} = 5\,\mu$m and $\alpha^{-1} = 25\,\mu$m, corresponding to the strongly absorbed or weakly absorbed cases, using Snell's law to compute the refraction angles, and Beer's law for the LWIR attenuation. As shown in Figs. 5(d) and 5(e), refraction causes the LWIR beam to be concentrated below the intersections of the normal plane and the oblique planes. With the strongly absorbed LWIR (Fig. 5(d)), most of which was absorbed near the surface, there was only a slight concentration effect. With the weakly absorbed LWIR (Fig. 5(e)) there was a significant LWIR concentration tens of microns below the surface. In fact at certain locations the weakly absorbed LWIR intensity was 1.8 times greater than the incident intensity. We ran another simulation where the RDX crystals were tilted slightly (10°) off normal incidence (Fig. 5(f)), to verify these LWIR concentration effects were not artifacts of precise normal incidence. As shown in Figs. 5(g) and 5(h), the LWIR concentration effect did not require normal incidence. The crystal planes create prisms that act as crude lenses to elliptically focus the incoming LWIR.

With the longer-duration, lower-intensity LWIR used here, the heat distribution in a homogeneous RDX slab would be nearly identical at strongly absorbed and weakly absorbed LWIR wavelengths. With oblique crystal planes, however, there is a focusing effect that is more significant with weakly absorbed LWIR. By itself the focusing effect would not strongly affect the RDX heat distribution: thermal diffusion would conduct most of the excess heat produced near the focal regions into the rest of the RDX. Thus we have to postulate an additional factor to explain our hot spot observations. We suggest that the enhanced hot spots with weakly absorbed LWIR result from LWIR interactions with the inclusion defects[14–16] in the RDX crystals. The focused weakly absorbed LWIR irradiates a larger crystal volume than the strongly absorbed LWIR, increasing the likelihood of irradiating an inclusion with an internally focused LWIR beam.

Indeed, such inclusions are well known in RDX crystals. RDX crystal growth by solvent evaporation was studied by Heijden and co-workers,[17] who found that acetone-grown crystals have prominent (200) faces with adjacent oblique planes.[17] Borne and co-workers[15] used optical microscopy to study RDX in various index-matching liquids. When the refractive index was 1.6, the crystal bulk became invisible and many micron-size roughly spherical internal defects, consisting of solvent inclusions,[14] air pockets, or impurities such as the related explosive HMX[16] were observed.

The inclusions may or may not be strongly absorbing in the LWIR. Inclusions that contained solvents or other impurities may well absorb LWIR more strongly than RDX.

This article is copyrighted as indicated in the article. Reuse of AIP content is subject to the terms at: http://scitation.aip.org/termsconditions. Downloaded to IP: 130.126.229.119 On: Tue, 11 Feb 2014 17:02:01

Alternatively, non-absorbing spherical inclusions of RDX could also create hot spots by acting as short focal length lenses to enhance the local LWIR intensity, or by creating multiple reflections that interfere constructively.

Using LWIR to irradiate RDX crystals, we have shown that weakly absorbed wavelengths create hot spots more efficiently than strongly absorbed wavelengths. This is true specifically when the LWIR pulses are long-duration and low intensity. If the LWIR pulses were intense and short in duration, so heating was adiabatic, then the RDX surfaces would be much hotter in the strongly absorbed LWIR regime. But with lower-intensity LWIR used here, the RDX surface temperatures do not depend on absorption coefficients. The oblique crystal planes provided a focusing effect that was stronger with weakly absorbed LWIR because it penetrated more deeply into RDX. The penetrating focused weakly absorbed LWIR has a greater likelihood of irradiating a defect inclusion within an RDX crystal than strongly absorbed LWIR, enhancing the ability of weakly absorbed LWIR to create hot spots. RDX is a model system that is representative of many widely used EM, and it is likely that similar LWIR effects would be present in other transparent dielectric EM.

The research described in this study was based on work supported by the US Office of Naval Research under Award No. N00014-11-1-0418, the US Air Force Office of Scientific Research under Award No. FA9550-09-1-0163, the Defense Threat Reduction Agency under Award No. HDTRA1-12-1-0011, and work supported in part by National Science Foundation award CHE 10-11972. We thank Dr. Dan Hooks from Los Alamos National Laboratory for providing the RDX.

[1]F. P. Bowden and A. D. Yoffe, *Initiation and Growth of Explosion in Liquids and Solids* (University Press, Cambridge, 1952).
[2]F. P. Bowden and A. D. Yoffe, *Fast Reactions in Solids* (Academic Press, Inc., New York, 1958).
[3]B. A. Khasainov, A. V. Attetkov, and A. A. Borisov, Chem. Phys. Rep. **15**, 987 (1996).
[4]J. E. Field, Acc. Chem. Res. **25**, 489 (1992).
[5]M. J. Gifford, W. G. Proud, and J. E. Field, Thermochim. Acta **384**, 285 (2002).
[6]M.-W. Chen, S. You, K. S. Suslick, and D. D. Dlott, "Hot spots in energetic materials generated by infrared and ultrasound, detected by thermal imaging microscopy," Rev. Sci. Instrum. (to be published).
[7]A. W. Campbell, W. C. Davis, J. B. Ramsay, and J. R. Travis, Phys. Fluids **4**, 511 (1961).
[8]J. T. Dickinson, L. C. Jensen, D. L. Doering, and R. Yee, J. Appl. Phys. **67**, 3641 (1990).
[9]M. D. Perry, B. C. Stuart, P. S. Banks, M. D. Feit, V. Yanovsky, and A. M. Rubenchik, J. Appl. Phys. **85**, 6803 (1999).
[10]J. Köhler and R. Meyer, *Explosives*, 4th ed. (VCH Publishers, New York, 1993).
[11]R. Infante-Castillo, L. Pacheco-Londoño, and S. P. Hernández-Rivera, Spectrochim. Acta A **76**, 137 (2010).
[12]E. Matthias, M. Reichling, J. Siegel, O. W. Käding, S. Petzoldt, H. Skurk, P. Bizenberger, and E. Neske, Appl. Phys. A **58**, 129 (1994).
[13]M. S. Miller, "Thermophysical properties of RDX," US Army Research Laboratory Technical Report ARL-TR-1319, DTIC, Fort Belvoir, VA, 1997.
[14]D.-Y. Kim, K.-J. Kim, and H.-S. Kim, Propell. Explos. Pyrotech. **35**, 38 (2010).
[15]L. Borne, M. Herrmann, and C. B. Skidmore, in *Energetic Materials. Particle Processing and Characterization*, edited by U. Teipel (Wiley-VCH, Weinheim, 2005), p. 333.
[16]L. Borne and H. Ritter, Propell. Explos. Pyrotech. **31**, 482 (2006).
[17]A. v. d. Heijden, J. ter Horst, J. Kendrick, K.-J. Kim, H. Kröber, F. Simon, and U. Teipel, in *Energetic Materials. Particle Processing and Characterization*, edited by U. Teipel (Wiley-VCH, Weinheim, 2005), p. 53.

This article is copyrighted as indicated in the article. Reuse of AIP content is subject to the terms at: http://scitation.aip.org/termsconditions. Downloaded to IP: 130.126.229.119 On: Tue, 11 Feb 2014 17:02:01